Dysfunctional d-aspartate metabolism in BTBR mouse model of idiopathic autism

Tommaso Nuzzo, Masae Sekine, Daniela Punzo, Mattia Miroballo, Masumi Katane, Yasuaki Saitoh, Alberto Galbusera, Massimo Pasqualetti, Francesco Errico, Alessandro Gozzi, et al.

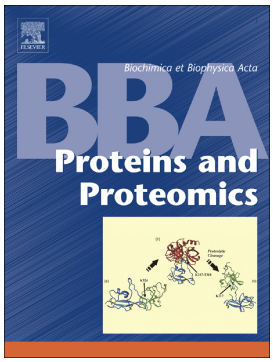

Dysfunctional d-aspartate metabolism in BTBR mouse model of idiopathic autism

Tommaso Nuzzo, Masae Sekine, Daniela Punzo, Mattia Miroballo, Masumi Katane, Yasuaki Saitoh, Alberto Galbusera, Massimo Pasqualetti, Francesco Errico, Alessandro Gozzi, Jean-Pierre Mothet, Hiroshi Homma, Alessandro Usiello

PII: S1570-9639(20)30178-3

DOI: https://doi.org/10.1016/j.bbapap.2020.140531

Reference: BBAPAP 140531

To appear in: *BBA - Proteins and Proteomics*

Received date: 16 May 2020

Revised date: 22 July 2020

Accepted date: 31 July 2020

Please cite this article as: T. Nuzzo, M. Sekine, D. Punzo, et al., Dysfunctional d-aspartate metabolism in BTBR mouse model of idiopathic autism, *BBA - Proteins and Proteomics* (2020), https://doi.org/10.1016/j.bbapap.2020.140531

Dysfunctional D-aspartate metabolism in BTBR mouse model of idiopathic autism

Tommaso Nuzzo[1], Masae Sekine[2], Daniela Punzo[3], Mattia Miroballo[1], Masumi Katane[2], Yasuaki Saitoh[2], Alberto Galbusera[4], Massimo Pasqualetti[5], Francesco Errico[6], Alessandro Gozzi[4], Jean-Pierre Mothet[7], Hiroshi Homma[2,@], Alessandro Usiello[1,3,8,@]

[1]Translational Neuroscience Unit, IRCCS "Casa Sollievo della Sofferenza", San Giovanni Rotondo, Italy;
[2]Graduate School of Pharmaceutical Sciences, Kitasato University, Tokyo, Japan;
[3]CEINGE Biotecnologie Avanzate, Naples, Italy;
[4]Functional Neuroimaging Laboratory, Istituto Italiano di Tecnologia, Center for Neuroscience and Cognitive Systems, Rovereto (TN), Italy;
[5]Department of Biology, Unit of Cell and Developmental Biology, University of Pisa, 56127 Pisa, Italy;
[6]Department of Agricultural Sciences, University of Naples "Federico II", Via Università, 100, 80055, Portici, Italy;
[7]Laboratoire LuMin, FRE 2036 CNRS, ENS Paris Saclay, Université Paris-Saclay, 91190 Gif-sur-Yvette, France;
[8]Department of Environmental, Biological and Pharmaceutical Sciences and Technologies, University of Campania "Luigi Vanvitelli", Caserta, Italy.

[@] **Corresponding authors**:

Hiroshi Homma, Graduate School of Pharmaceutical Sciences, Kitasato University, Tokyo, Japan. email: hommah@pharm.kitasato-u.ac.jp

Alessandro Usiello, Department of Environmental, Biological and Pharmaceutical Sciences and Technologies, University of Campania "Luigi Vanvitelli", Via A. Vivaldi, 4, 81100 Caserta, Italy. email: usiello@ceinge.unina.it.

Current Affiliations:

Tommaso Nuzzo, Department of Environmental, Biological and Pharmaceutical Sciences and Technologies, University of Campania "Luigi Vanvitelli", Via A. Vivaldi, 4, 81100 Caserta, Italy.

Daniela Punzo, Department of Microbiology & Molecular Genetics, U1233 INSERM, Center for Epigenetics and Metabolism, University of California, Irvine, Irvine, CA 92697, USA.

Alessandro Usiello, since 2020 is no longer affiliated with Translational Neuroscience Unit, IRCCS "Casa Sollievo della Sofferenza", San Giovanni Rotondo, Italy

Abstract

Background

Autism spectrum disorders (ASD) comprise a heterogeneous group of neurodevelopmental conditions characterized by impairment in social interaction, deviance in communication, and repetitive behaviors. Dysfunctional ionotropic NMDA and AMPA receptors, and metabotropic glutamate receptor 5 activity at excitatory synapses has been recently linked to multiple forms of ASD. Despite emerging evidence showing that D-aspartate and D-serine are important neuromodulators of glutamatergic transmission, no systematic investigation on the occurrence of these D-amino acids in preclinical ASD models has been carried out.

Methods

Through HPLC and qPCR analyses we investigated D-aspartate and D-serine metabolism in the brain and serum of four ASD mouse models. These include BTBR mice, an idiopathic model of ASD, and *Cntnap2*$^{-/-}$, *Shank3*$^{-/-}$, and *16p11.2*$^{+/-}$ mice, three established genetic mouse lines recapitulating high confidence ASD-associated mutations.

Results

Biochemical and gene expression mapping in *Cntnap2*$^{-/-}$, *Shank3*$^{-/-}$, and *16p11.2*$^{+/-}$ failed to find gross cerebral and serum alterations in D-aspartate and D-serine metabolism. Conversely, we found a striking and stereoselective increased D-aspartate content in the prefrontal cortex, hippocampus and serum of inbred BTBR mice. Consistent with biochemical assessments, in the same brain areas we also found a robust reduction in mRNA levels of *D-aspartate oxidase*, encoding the enzyme responsible for D-aspartate catabolism, and an increased mRNA expression of *serine racemase*, which is partially involved in cerebral D-aspartate biosynthesis.

Conclusions

Our results demonstrated the presence of disrupted D-aspartate metabolism in a widely used animal model of idiopathic ASD.

General Significance

Overall, this work calls for a deeper investigation of D-amino acids in the etiopathology of ASD and related developmental disorders.

Keywords: D-aspartate, D-aspartate oxidase, NMDA receptors, D-serine, Autism Spectrum Disorder.

1. Introduction

Autism spectrum disorder (ASD) is characterized by severe and sustained impairment in social interaction, deviance in communication, and repetitive behaviors [1, 2]**.** The causes of ASD vary greatly, including both genetic and environmental factors. A remarkable preponderance of ASD-associated genetic mutations affect proteins mediating synaptic functions, such as SH3 and multiple ankyrin repeat domains 3 (SHANK3), contactin-associated protein-like (CNTNAP), neuroligins, and neurexins [3-6]. Other genetic aberrations associated with ASD include copy number variations (CNVs) in chromosomal loci 15q11-q13, 16p11.2, and 22q11.21 [5, 7].

A large body of evidence points at impaired glutamatergic signaling in ASD [8-14]. In keeping with this, clinical studies have identified several genetic variations in L-glutamate (L-Glu) ionotropic receptor NMDA type (NMDAR) subunit 2A and 2B (*GRIN2A* and *GRIN2B*), as well as in other genes of the metabotropic L-Glu receptor (mGluR) network in ASD patients [11, 12]. Moreover, positive and negative NMDAR modulators and mGluR5 antagonists have been shown to alleviate ASD symptoms in patients and normalize ASD-like phenotypes in animal models [11]**.** These results suggest that both hyper- and hypoactivation of these receptors might induce ASD-like symptoms. Altered NMDAR functions have been also reported in a number of rodent models of syndromic forms of ASD, including *Shank3*$^{\Delta C/\Delta C}$ mice, *Neuroligin-3*^{R451C} knock-in mice, and *Fmr1*$^{-/-}$ mice [15], as well as in mice and rats prenatally exposed to valproic acid [16, 17], a teratogen known to induce ASD in humans.

Recently, several lines of evidence have shown that changes (e.g., availability, metabolism, and/or receptor activity) in neuroactive free amino acids may play a role in the pathogenesis and/or pharmacotherapy of severe psychiatric disorders characterized by a developmental origin (e.g., schizophrenia) and sharing symptoms with ASD, including cognitive and social interaction impairments [18-24]. Among these amino acids, free D-serine (D-Ser) and D-aspartate (D-Asp) act as co-agonist and agonist for NMDARs, respectively [25-27]. Moreover, D-Asp has also been shown to activate mGluR5-dependent transmission [28]. Remarkably, in mammalian brain D-Asp display a peculiar time-dependent occurrence, since it is highly abundant only at embryonic stages of life [29-31]. D-Ser is synthesized *de novo* by serine racemase (SR) [32, 33], while the metabolic pathway responsible for D-Asp biosynthesis has not yet been clearly defined [34-36]. However, some evidence has shown that SR might contribute to endogenous D-Asp formation [34, 35]. D-Ser and D-Asp are catabolized by two different peroxisomal enzymes, D-amino acid oxidase (DAAO) [37, 38] and D-aspartate oxidase (DDO) [27, 39], respectively. Although several studies indicate that D-Asp and D-Ser might be involved in the pathogenesis of psychiatric disorders such as schizophrenia [20, 27, 40-43], bipolar disorder [44, 45], and depression [46-48], the role of these D-amino acids in ASD has not yet been addressed. Here, for the first time, we investigated the metabolism of D-Asp and D-Ser in the brain and serum of four well-established animal models of ASD, including BTBR T+ Itpr3tf/J (BTBR) [49], *Cntnap2*$^{-/-}$ [50], *Shank3*$^{-/-}$ [51], and *16p11.2*$^{+/-}$ [52] mice.

2. Materials and Methods

2.1. Animals and ethical statement

Adult mice of the inbred strains C57BL/6J and BTBR along with *Cntnap2*$^{-/-}$, *Shank3*$^{-/-}$, and *16p11.2*$^{+/-}$ with their relative control "wild-type" breeding pairs were obtained from Jackson Laboratory (Bar Harbor, ME, USA). Animal studies were conducted in accordance with Italian Law (DL 26/2014, EU 63/2010, Ministero della Sanità, Roma) and recommendations outlined in the Guide for the Care and Use of Laboratory Animals of the National Institutes of Health. Mice were housed by sex in mixed genotype groups, with temperature maintained at 21 ± 1 °C and humidity at 60 ± 10%. All experiments were performed on adult male mice at the age of 3-4 months. All surgical procedures were performed under anesthesia. Serum samples were obtained through retro-orbital blood sampling before euthanizing the animals. Once the animals were sacrificed, prefrontal cortex and hippocampus were dissected out within 20s on an ice-cold surface and stored at -80°C for further experiments.

2.2. Serum extraction

After retro-orbital sampling, blood was collected in microtubes and left for 1 h at room temperature and then centrifuged (1500 rpm, 10 min 4°C) for serum separation. Red blood cell hemolysis was evaluated by direct observation [53].

2.3. HPLC analysis of amino acids content in brain and serum

Brain samples were homogenized in 200 µL of PBS and centrifuged at 20,000 × *g* for 15 min at 4°C. Subsequently, 10 µL of 40 w/v % trichloroacetic (TCA) and 150 µL of water were added to 150 µL of the supernatant, and the mixture was stored at 4°C for 10 min. Precipitated proteins were then removed by centrifugation at 20,000 × *g* for 15 min at 4°C. To 150 µL of the supernatant, 100 µL of 200 mM sodium borate buffer (pH 8.0), 20 µL of 1 M NaOH, and 130 µL of water were added and mixed well. Then, 20 µL of the mixture was mixed with 40 µL of 50 mM sodium borate buffer (pH 8.5) and 50 µL of 10 mM 4-fluoro-7-nitrobenzofurazan (NBD-F) in dry acetonitrile and incubated at 60°C for 5 min

for fluorescence derivatization of free amino acids. After stopping the derivatization reaction by adding 890 µL of 1% trifluoroacetic acid, 10 µL of the sample solution was injected into the HPLC system as described below after filtration through a 0.45-µm membrane filter. NBD-D- and L-Asp as well as NBD-D- and L-Ser were separated and fluorometrically detected by essentially following previously reported method [54]. In the case of NBD-D, L-Asp, columns of InertSustain C8 (250 × 4.6 mm, i.d., 5 µm, GL Sciences Inc., Tokyo, Japan) and Sumichiral OA-3200 (250 × 4.6 mm, i.d., 5 µm, Sumika Analytical Center, Osaka, Japan) were used as a reversed-phase octylsilyl silica gel column and a Pirkle-type chiral column, respectively. Column temperature was 35°C. The mobile phases used were 10 mM sodium citrate (pH 5.0): methanol = 88:12 (v/v) (0.8 mL/min) for the octylsilyl silica gel column and 8 mM citrate in methanol:acetonitrile = 95:5 (0.8 mL/min) for the chiral column, respectively. For NBD-D, L-Ser, the columns were the same as for NBD-D, L-Asp. The mobile phases used were 20 mM sodium citrate (pH 6.0): methanol = 88:12 (v/v) (0.8 mL/min) for the octylsilyl silica gel column and 5 mM citrate in methanol : acetonitrile = 95:5 (0.8 mL/min) for the chiral column, respectively. Brain samples were also analyzed for L-Glu content, as previously described [55]. Prefrontal cortex (PFC) and hippocampus samples were homogenized in 1:10 (w/v) 0.2 M TCA, sonicated (3 cycles, 10 s each), and centrifuged at 13,000 x *g* for 20 min. All the precipitated protein pellets from brain samples were stored at -80 °C for protein quantification. TCA supernatants were then neutralized with 0.2 M NaOH and subjected to precolumn derivatization with o-phthaldialdehyde/N-acetyl-L-cysteine. Diastereoisomer derivatives were resolved on a Simmetry C8 5-µm reversed-phase column (Waters, 4.6x250 mm). Identification and quantification were based on retention times and peak areas and compared with those associated with external standards. The detected L-Glu levels in the serum were expressed as µM.

Serum samples were analyzed for D-Asp, L-Asp, D-Ser, L-Ser, and L-Glu, as previously reported [55]. Here, 100 µl serum samples were mixed in a 1:10 dilution with HPLC-grade methanol (900 µl) and

centrifuged at 13,000 x *g* for 10 min. Supernatants were dried, suspended in 0.2 M TCA, and then neutralized with 0.2 M NaOH. Samples were then subjected to precolumn derivatization with o-phthaldialdehyde (OPA)/N-acetyl-L-cysteine in 50% methanol. Diastereoisomer derivatives were resolved on a Simmetry C8 5-µm reversed-phase column (Waters, 4.6x250 mm) under isocratic conditions (0.1 M sodium acetate buffer, pH 6.2, 1% tetrahydrofuran, and 1 ml/min flow rate). A washing step in 0.1 M sodium acetate buffer, 3% tetrahydrofuran, and 47% acetonitrile was performed after every single run. Identification and quantification of D-Ser, L-Ser, D-Asp, L-Asp, and L-glutamate (L-Glu) were based on retention times and peak areas and compared with those associated with external standards. The identity of peaks was confirmed by adding known amounts of external standards. The identity of the D-Asp peak was also evaluated by selective degradation catalyzed by a recombinant human DDO (hDDO) [56, 57]; briefly, hDDO enzyme (12.5 µg) was added to the samples, incubated at 30 °C for 3 hours, and subsequently derivatized. Amino acid levels were expressed as µM, while the D-/total amino acid ratio was expressed as percentage (%).

2.4. RNA extraction and qRT-PCR

Total RNA was extracted by using the RNeasy mini kit (QIAGEN) according to the manufacturer's instructions. The integrity of the RNA was assessed by denaturing agarose gel electrophoresis (presence of sharp 28S, 18S, and 5S bands) and spectrophotometry (NanoDrop 2000, Thermo Scientific). Total RNA was purified to eliminate potentially contaminating genomic DNA using recombinant DNase (QIAGEN). A total of 1 µg of total RNA of each sample was reverse-transcribed with Quanti Tect Reverse Transcription (QIAGEN) using oligo-dT and random primers mix according to the manufacturer's instructions. qRT-PCR amplifications were performed using LightCycler 480 SYBR Green I Master (Roche Diagnostic) in a LightCycler480 Real Time thermocycler (Roche). The following protocol was used: 10 s for initial denaturation at 95°C followed by 40 cycles consisting of

10 s at 94°C for denaturation, 10 s at 60°C for annealing, and 6 s for elongation at 72°C. The following primers were used for mouse *Ddo, Daao, Sr* cDNA amplification: *Ddo* forward 5-ACCACCAGTAATGTAGCGGC-3 and *Ddo* reverse 5-GGTACCGGGGTATCTGCAC-3; *Daao* forward 5-TTTTCTCCCGACACCTGGC-3 and *Daao* reverse 5-TGAACGGGGTGAATCGATCT-3; *Sr* forward 5-CCCTTGGTAGATGCACTGGT and *Sr* reverse 5-TCAGCAGCGTATACCTTCACAC-3. β-actin and PP1A were used as housekeeping genes for PCR: β-actin forward 5-CTAAGGCCAACCGTGAAAAG-3 and β-actin reverse 5-ACCAGAGCATACAGGGACA-3, PP1A forward 5-GTGGTCTTTGGGAAGGTGAA-3 and PP1A reverse 5-TTACAGGACATTGCGAGCAG-3.

2.5 Statistical analysis

Statistical analysis of HPLC detections was performed using Aspin-Welch's test, given the high variance heterogeneity of data. qPCR experiments were analyzed by unpaired Student's *t*-test. Correlation analyses were calculated using Pearson's correlation. All *p* values less than 0.05 were considered statistically significant.

3. Results

3.1. D-aspartate and L-aspartate content in the prefrontal cortex of ASD mouse models.

HPLC measurements revealed a dramatic increase in D-Asp levels in PFC of BTBR mice, compared to the C57BL/6J mice used as the control strain (PFC: C57BL/6J = 44.24±8.71 nmol/g tissue vs BTBR = 148.40±27.60 nmol/g tissue, p=0.027; Aspin-Welch's test; Figure 1a). In contrast to D-Asp, the amount of L-Asp was not significantly altered in of BTBR mice when compared to the C57BL/6J

group (C57BL/6J = 3635±732 nmol/g tissue vs BTBR = 2642±550 nmol/g tissue, p=0.323; Aspin-Welch's test; Figure 1b). Thus, consistent with the selective increase in D-Asp content, the D-Asp/total Asp (D+L) ratio was significantly higher in BTBR mice than in controls. (C57BL/6J = 1.21±0.05 % vs BTBR = 5.38±0.25 %, p<0.0001; Aspin-Welch's test; Figure 1c).

HPLC analysis performed in *Cntnap2*$^{-/-}$ animals showed similar cortical levels of both D-Asp and L-Asp, compared to the *Cntnap2*$^{+/+}$ mice, used as the control group (D-Asp: p=0.523; L-Asp: p=0.670; Aspin-Welch's test; Figure 1d,e). As a result, the D-Asp/total Asp ratio did not significantly change between groups (p=0.083; Figure 1f).

In *Shank3*$^{-/-}$ mice, we did not observe any significant difference compared to the *Shank3*$^{+/+}$ group in the amount of D-Asp and L-Asp, and D-Asp/total Asp ratio, (D-Asp, p=0.192; L-Asp, p=0.151; D-/total Asp, p=0.183; Aspin-Welch's test; Figure 1g-i).

Like *Shank3*$^{-/-}$, also the *16p11.2*$^{+/-}$ brains showed similar levels of D-Asp, L-Asp, and D-Asp/total Asp ratio compared to the control *16p11.2*$^{+/+}$ group (PFC: D-Asp, p=0.756; L-Asp, p=0.838; D-/total Asp ratio, p=0.339; Figure 1j-l).

Taken together, these HPLC data highlight a prominent increase in D-Asp levels within the PFC of BTBR mice. Conversely, no gross alterations in these amino acid levels were documented in the PFC of *Cntnap2*$^{-/-}$, *Shank3*$^{-/-}$ and *16p11.2*$^{+/-}$ mutants when compared to their matched controls.

3.2. D-aspartate and L-aspartate content in the hippocampus of ASD mouse models.

Consistent with PFC data, HPLC analysis revealed a strong increase in D-Asp levels but not in L-Asp content in the hippocampus of BTBR mice, compared to the C57BL/6J mice (D-Asp: C57BL/6J = 46.84±13.40 nmol/g tissue vs BTBR = 187.10±36.46 nmol/g tissue, p=0.025; L-Asp: C57BL/6J = 4616.00±1383.00 nmol/g tissue vs BTBR = 4394.00±938.40 nmol/g tissue, p=0.899; Aspin-Welch's test; Figure 2a,b). In line with the selective increase in D-Asp content, the D-Asp/total Asp ratio was

significantly higher in the hippocampus of BTBR mice compared to controls (C57BL/6J = 1.04±0.06 % vs BTBR = 4.15±0.15 %, $p<0.0001$; Aspin-Welch's test; Figure 2c). Furthermore, we found a positive correlation between cortical and hippocampal D-Asp content in BTBR (Pearson's correlation, $r=0.942$, $p=0.058$; data not shown), but not in C57BL/6J animals (Pearson's correlation, $r=-0.182$, $p=0.818$; data not shown).

In contrast to the unaltered cortical levels of Asp enantiomers, HPLC data indicated a trend to decrease of ~50% in the amount of both D-Asp and L-Asp in the hippocampus of *Cntnap2*$^{-/-}$ mice, compared to *Cntnap2*$^{+/+}$ mice (D-Asp: *Cntnap2*$^{+/+}$ = 59.63±10.79 nmol/g tissue vs *Cntnap2*$^{-/-}$ = 29.93±5.41 nmol/g tissue, $p=0.064$; L-Asp: *Cntnap2*$^{+/+}$ = 5859±1012 nmol/g tissue vs *Cntnap2*$^{-/-}$ = 2844.00±320.60 nmol/g tissue, $p=0.053$; Aspin-Welch's test; Figure 2d,e). Consistent with a comparable reduction in both Asp enantiomers, we found a comparable D-Asp/total Asp ratio between genotypes ($p=0.842$; Aspin-Welch's test; Figure 2f).

In *Shank3*$^{-/-}$ mice, we found unaltered levels of D-Asp and L-Asp, and D-Asp/total Asp ratio compared to the *Shank3*$^{+/+}$ group (D-Asp, $p=0.832$; L-Asp, $p=0.861$; D-Asp/total Asp ratio, $p=0.488$; Figure 2g-i). Similarly, *16p11.2*$^{+/-}$ mice hippocampus showed similar levels of D-Asp, L-Asp, and D-Asp/total Asp ratio compared to the control *16p11.2*$^{+/+}$ group (D-Asp, $p=0.585$; L-Asp, $p=0.874$; D-/total Asp ratio, $p=0.122$; Figure 2j-l).

Overall, like PFC, we reported a prominent increase in D-Asp levels within the hippocampus of BTBR mice. In addition, we revealed significantly reduced D-Asp and L-Asp content in the hippocampus of *Cntnap2*$^{-/-}$ mice. In contrast, no significant changes in these amino acid levels were detected in *Shank3*$^{-/-}$ and *16p11.2*$^{+/-}$ animals when compared to their matched controls.

3.3. D-serine and L-serine levels in the prefrontal cortex and hippocampus of ASD mouse models

Neurochemical experiments indicate that, despite there being no gross alterations in either D-Ser or L-Ser levels in PFC homogenates of BTBR animals (D-Ser: p=0.871; L-Ser: p=0.875; Aspin-Welch's test; Table 1), a mild reduction was found in the D-Ser/total Ser ratio when compared to the C57BL/6J control animals (C57BL/6J= 31.74±0.45 % vs BTBR = 29.36±0.45 %, p=0.009; Aspin-Welch's test; Table 1). Conversely, in the hippocampus of BTBR, the amounts of D-Ser and L-Ser (D-Ser: p=0.351; L-Ser: p=0.335; Aspin-Welch's test; Table 1) as well as the D-Ser/total Ser ratio were comparable to those measured in C57BL/6J brains (p=0.393; Aspin-Welch's test; Table 1). Besides no evident D-Ser alterations, we found a positive correlation between D-Ser and D-Asp levels within PFC and hippocampus of both BTBR (Pearson's correlation, PFC: r=0.978, p=0.022; hippocampus: r=0.961, p=0.039; data not shown) and C57BL/6J (Pearson's correlation, PFC: r=0.965, p =0.035; hippocampus: r=0.998, p=0.002; data not shown) mice.

In the PFC of *Cntnap2*$^{-/-}$, HPLC analysis did not indicate any evident change in the amounts of D-Ser and L-Ser or in the D-Ser/total Ser ratio when compared to those measured in the control group (D-Ser: p=0.597; L-Ser: p=0.566; D-Ser/total Ser: p=0.631; Aspin-Welch's test; Table 1). In contrast to the PFC, we revealed a decreasing trend in the amounts of both D-Ser and L-Ser in the hippocampus of *Cntnap2*$^{-/-}$ mutants compared to controls (D-Ser: p=0.085; L-Ser: p=0.101; Aspin-Welch's test; Table 1). Consistent with D-Ser and L-Ser levels, D-Ser/total Ser ratio was comparable between genotypes (p=0.447; Aspin-Welch's test; Table 1).

In *Shank3*$^{-/-}$ brains, cortical D-Ser levels tended to slightly increase compared to *Shank3*$^{+/+}$ control mice (p=0.160; Aspin-Welch's test; Figure 2m), while comparable L-Ser content and D-Ser/total Ser ratio were found between genotypes (L-Ser: p=0.284; D-Ser/total Ser ratio: p=0.693; Aspin-Welch's test; Table 1). In the hippocampus of *Shank3*$^{-/-}$ mice we detected no differences in D-Ser and L-Ser content and D-Ser/total Ser ratio as compared to *Shank3*$^{+/+}$ animals (D-Ser: p=0.937; L-Ser: p=0.930; D-/total Ser ratio: p=0.542; Aspin-Welch's test; Table 1).

Finally, we did not observe any gross alterations in D-Ser and L- Ser cerebral levels or in the D-Ser/total Ser ratio in either the PFC or hippocampus of *16p11.2*$^{+/-}$ mice when compared to *16p11.2*$^{+/+}$control animals (PFC: D-Ser, p=0.540; L-Ser, p=0.480; D-/total Ser ratio, p=0.744; hippocampus: D-Ser, p=0.534; L-Ser, p=0.540; D-/total Ser ratio, p=0.723; Aspin-Welch's test; Table 1).

In conclusion, HPLC data indicate that D-Ser and L-Ser levels were only mildly altered within the PFC and hippocampus of *BTBR, Cntnap2*$^{-/-}$, *Shank3*$^{-/-}$ *and 16p11.2*$^{+/-}$ animal models of ASD.

3.4. D-aspartate, L-aspartate and D-serine, L-serine concentrations in the serum of ASD mouse models

Using HPLC, we also investigated levels of D-Asp, D-Ser, and their respective L-enantiomers in the serum of adult *BTBR*, *Cntnap2*$^{-/-}$, *Shank3*$^{-/-}$, and *16p11.2*$^{+/-}$ mice.

Consistent with the cerebral measurements, we found a dramatic increase in D-Asp levels and D-Asp/total Asp ratio in the serum of BTBR mice, compared to C57BL/6J animals (D-Asp: C57BL/6J = 0.56±0.29 μM vs BTBR = 2.99±0.54 μM, p=0.012; D-Asp/total Asp ratio: C57BL/6J = 3.12±0.96 % vs BTBR = 10.23±2.06 %, p=0.023; Aspin-Welch's test; Figure 3a, c). Notably, unlike the brain, we also observed a trend to increase in L-Asp amount in the serum of BTBR mice than in the controls (C57BL/6J =14.65±4.03 μM vs BTBR=26.76±2.91 μM, p=0.055; Aspin-Welch's test; Figure 3b).

We did not find any significant alterations in either D-Ser or L-Ser serum concentrations of BTBR mice (D-Ser, p=0.224; L-Ser, p=0.384; Aspin-Welch's test; Table 1). However, a mild increase in D-Ser/total Ser ratio was observed in BTBR mice when compared to C57BL/6J animals (p=0.053; Aspin-Welch's test; Table 1).

Moreover, we detected comparable serum D-Asp and L-Asp levels and D-Asp/total Asp ratio in *Cntnap2*$^{-/-}$ mutants as compared to *Cntnap2*$^{+/+}$ controls (D-Asp, p=0.216; L-Asp, p=0.679; D-Asp/total

Asp ratio, p=0.153; Figure 3d-f). Notably, although no gross changes were observed in the serum D-Ser and L-Ser levels in *Cntnap2*$^{-/-}$ mice (D-Ser, p=0.842; L-Ser, p=0.287; Aspin-Welch's test; Table 1), we detected significantly decreased D-Ser/total Ser ratio in these mutants as compared to their controls (*Cntnap2*$^{+/+}$= 1.87±0.12 % vs *Cntnap2*$^{-/-}$ = 1.40±0.12 %, p=0.036; Aspin-Welch's test; Table 1).

Moreover, we found comparable serum D-Asp and L-Asp concentrations and D-Asp/total Asp ratio between *Shank3*$^{-/-}$ and *Shank3*$^{+/+}$ mice (D-Asp, p=0.792; L-Asp, p=0.474; D-/total Asp ratio, p=0.767; Aspin-Welch's test; Figure 3g-i). Similarly, serum D-Ser and L-Ser levels and D-Ser/total Ser ratio were also unaltered in these mutant mice (D-Ser, p=0.636; L-Ser, p=0.839; D-/total Ser ratio, p=0.573; Aspin-Welch's test; Table 1).

We found no differences in the serum D-Asp, L-Asp, D-Ser, and L-Ser concentrations in *16p11.2*$^{+/-}$ mice as compared to *16p11.2*$^{+/+}$ controls (D-Asp, p=0.351; L-Asp, p=0.537; D-Ser, p=0.187; L-Ser, p=0.581; Figure 3j,k; Aspin-Welch's test; Table 1). Additionally, D-Asp/total Asp and D-Ser/total Ser ratios were not statistically different between genotypes (D-Asp/total Asp ratio, p=0.229; D-Ser/total Ser ratio, p=0.208; Aspin-Welch's test; Figure 3l; Table 1).

Overall, HPLC experiments performed in the serum confirmed the existence of dramatically increased D-Asp levels in BTBR animals, along with a significant reduction in D-Asp/total Asp ratio in *Cntnap2*$^{-/-}$ mutant mice. In contrast, no statistical differences in D-Asp, L-Asp and D-Ser, L-Ser levels were documented in *Shank3*$^{-/-}$ and *16p11.2*$^{+/-}$ mutants when compared to their matched controls.

3.5. L-glutamate content in the cortex, hippocampus, and serum of ASD mouse models

We measured the content of L-Glu in the PFC, hippocampus, and serum of BTBR, *Cntnap2*$^{-/-}$, *Shank3*$^{-/-}$ and *16p11.2*$^{+/-}$ mice. Our HPLC analysis did not find any significant differences in L-Glu levels in the PFC of BTBR, *Cntnap2*$^{-/-}$ and *16p11.2*$^{+/-}$ mice compared to the respective control mice (BTBR, p=0.645; *Cntnap2*$^{-/-}$, p=0.915; *16p11.2*$^{+/-}$, p=0.462; Aspin-Welch's test; Figure 4a,b,d). Similarly, we

found no statistically significant changes in *Shank3*$^{-/-}$ mice, although a trend to decrease in L-Glu levels appeared, as compared to *Shank3*$^{+/+}$ animals (p=0.060; Aspin-Welch's test; Figure 4c).

In contrast to PFC, HPLC experiments showed a significant reduction in L-Glu concentration within the hippocampus of BTBR mice compared to C57BL/6J animals (C57BL/6J=6149±427 nmol/g tissue vs BTBR = 4841±182 nmol/g tissue, p=0.027; Aspin-Welch's test; Figure 4e). On the other hand, comparable L-Glu levels were found in the hippocampus of *Cntnap2*$^{-/-}$, *Shank3*$^{-/-}$, and *16p11.2*$^{+/-}$ mutants when compared to their matched controls (*Cntnap2*$^{-/-}$, p=0.131; *Shank3*$^{-/-}$, p=0.496; *16p11.2*$^{+/-}$, p=0.168; Aspin-Welch's test; Figure 4f,g,h).

Finally, we measured the serum L-Glu levels in all different mice strains. Notably, we found increased L-Glu levels in BTBR mice compared to C57BL/6J animals (C57BL/6J= 37.08±11.00 µM vs BTBR = 85.74±4.94, p=0.014; Aspin-Welch's test; Figure 4i). Conversely, serum L-Glu concentrations were unaltered between *Cntnap2*$^{-/-}$, *Shank3*$^{-/-}$, and *16p11.2*$^{+/-}$ mutants and their matched controls (*Cntnap2*$^{-/-}$, p=0.708; *Shank3*$^{-/-}$, p=0.326; *16p11.2*$^{+/-}$, p=0.452; Aspin-Welch's test; Figure 4j,k,l).

Taken together, these data indicate a robust increase in L-Glu levels in the serum of BTBR, while no alterations were detected in the PFC, hippocampus, and serum of *Cntnap2*$^{-/-}$, *Shank3*$^{-/-}$, and *16p11.2*$^{+/-}$ mice.

3.6. Altered Ddo and Sr mRNA expression in the brain of BTBR mice

Here, we analyzed the mRNA levels of the genes involved in the regulation of D-Asp and D-Ser synthesis and degradation. To this aim, we conducted qRT-PCR to determine the transcript levels of *Ddo*, *Daao*, and *Sr* in both the PFC and hippocampus of BTBR, *Cntnap2*$^{-/-}$, *Shank3*$^{-/-}$, and *16p11.2*$^{+/-}$ and matched control mice.

In line with the dramatic increase in D-Asp content, we found a robust reduction in *Ddo* transcript levels in both the PFC and hippocampus of BTBR mice compared to C57BL/6J animals (PFC,

p<0.0001; hippocampus, p<0.0001; Figure 5 a, d). Conversely, no significant alterations in *Ddo* gene expression were observed in either the PFC or hippocampus of *Cntnap2*$^{-/-}$, *Shank3*$^{-/-}$, and *16p11.2*$^{+/-}$ mice compared with their respective controls (PFC: *Cntnap2*$^{-/-}$, p=0.2602; *Shank3*$^{-/-}$, p=0.082; *16p11.2*$^{+/-}$, p=0.524; hippocampus: *Cntnap2*$^{-/-}$, p=0.1771; *Shank3*$^{-/-}$, p=0.663; *16p11.2*$^{+/-}$, p=0.884; unpaired Student's t-test; Figure 5g,j,m,p,s,v).

The analysis of *Daao* mRNA levels revealed that this transcript was almost undetectable in all the brain samples analyzed, even after 40 PCR cycles (Figure 5b,e,h,k,n,q,t,w).

On the other hand, qPCR analysis of *Sr* gene expression revealed unaltered mRNA levels in the PFC of BTBR mice, compared to C57BL/6J animals (p=0.149; unpaired Student's t-test; Figure 5c); however, a statistically significant increase was detected in the hippocampus of these animals (p=0.005; unpaired Student's t-test; Figure 5f). Conversely, in *Shank3*$^{-/-}$ mice, we observed reduced *Sr* mRNA levels in the PFC but not in the hippocampus (PFC, p=0.023; hippocampus, p=0.406; unpaired Student's t-test; Figure 5o, r). Finally, we found unaltered *Sr* transcripts within the PFC and hippocampus of both *Cntnap2*$^{-/-}$ and *16p11.2*$^{+/-}$ mice compared to matched controls (PFC: *Cntnap2*$^{-/-}$, p=0.158; *16p11.2*$^{+/-}$, p=0.831; hippocampus; *Cntnap2*$^{-/-}$, p=0.401; *16p11.2*$^{+/-}$, p=0.681; unpaired Student's t-test; Figure 5i,l,u,x).

Overall, these qPCR experiments highlight a dramatic reduction in *Ddo* mRNA expression within the PFC and hippocampus of BTBR mice, along with a significant increase in *Sr* transcripts in the hippocampus of the same animals. On the other hand, no gross changes in genes regulating D-amino acids metabolism were found in *Cntnap2*$^{-/-}$, *Shank3*$^{-/-}$, or *16p11.2*$^{+/-}$ animals when compared to matched controls.

4. Discussion

It is well known that dysregulated glutamatergic signaling is involved in the etiology of ASD [8-14]. Several studies in mouse models of ASD have shown abnormalities in synaptic plasticity due to dysfunctions in the NMDAR and AMPAR systems [58]. Pharmacological evidence in mouse models with deletions in synaptic genes *Fmr1*, *Mecp2*, and *Shank2*, and in the inbred BTBR strain also supports the hypothesis of altered glutamatergic transmission since treatment with glutamatergic drugs, including memantine, has demonstrated favorable outcomes [59-61]. In parallel to preclinical research, studies in ASD patients reported significantly increased serum and plasma glutamate concentrations, compared to healthy subjects [62-64]. Accordingly, a *post-mortem* study has shown augmented glutamate and glutamine content in the anterior cingulate cortex of a small cohort of seven individuals with autism [65].

Here, we explored the putative implication of an altered metabolism of the NMDAR modulators, D-Asp and D-Ser, in the physiopathology of ASD. We evaluated the cerebral content of these D-amino acids in different genetic mouse models of ASD, such as knockout mice for *Cntnap2* (*Cntnap2*$^{-/-}$; [4]), *Shank3B* (*Shank3*$^{-/-}$; [6]), and heterozygous mice with *16p11.2* deletion (*16p11.2*$^{+/-}$; [7]). Noteworthy, all these animal models show core ASD-like brain and behavioral deficits at the age of our biochemical characterization [50-52]. In addition to these syndromic models, we also analyzed BTBR mice, an idiopathic animal model of ASD [49, 66-68]. Although genetic and molecular abnormalities causing behavioral deficits in BTBR mice remain unclear [49, 69], this inbred mouse strain incorporates behavioral phenotypes relevant to all diagnostic symptoms of ASD, including reduced social interactions in juveniles and adults, repetitive self-grooming, and an unusual pattern of ultrasonic vocalizations resembling the atypical vocalizations that some autistic children produce [70, 71]. Moreover, BTBR mice show a severely reduced hippocampal commissure and absent corpus callosum [72], along with dysfunctional dopamine D2 receptor striatal neurotransmission and blunted

mesolimbic activity [73]. Of note, corpus callosum abnormalities have been also reported in autistic individuals [74, 75].

Here, we document a severe, dysfunctional D-Asp metabolism in BTBR brain (Table 2). Indeed, we found a very prominent increase in D-Asp content along with a severe reduction in *Ddo* gene expression in both the PFC and hippocampus of BTBR animals, compared to the same brain regions of C57BL/6J mice (Table 2). In agreement with this observation, previous transcriptome profiling identified *Ddo* among the 580 downregulated genes in the hippocampus of BTBR adult mice [76]. We also detected increased *Sr* transcript levels in BTBR hippocampus. This gene, encoding the enzyme responsible for D-Ser biosynthesis [77], has been suggested to take part also in cerebral D-Asp production [34-36]. Nevertheless, since 1) D-Ser levels are unchanged in the hippocampus of BTBR mice compared to controls, and 2) SR enzyme displays a much higher activity on the synthesis of D-Ser compared to D-Asp [35], it seems unlikely that the observed increase in *Sr* gene expression contributes to D-Asp elevation in this brain region of BTBR mice. Future studies will help to clarify whether *Sr* mRNA changes turn into altered SR protein levels and enzymatic activity in BTBR hippocampus. In line with these findings, we also report higher D-Asp concentrations in the serum of the BTBR strain than in the control mice. In this regard, it will be mandatory to evaluate the potential relevance of D-Asp as a novel biomarker for diagnostic measurements in idiopathic forms of ASD. Consistent with the agonism activity of D-Asp on NMDARs [27], we hypothesize that the altered D-Asp metabolism found in BTBR brain could influence NMDAR-dependent functions in this widely used idiopathic animal model of ASD [49, 66-68]. Yet, D-Asp is an agonist of mGluR5 [28] and, therefore, any increase in its levels should boost these receptors and, consequently, NMDARs function.

Previous studies have investigated the influence of increased endogenous D-Asp content in knockout mice for *Ddo* gene, an animal model backcrossed to C57BL/6J strain [78]. In line with well-established detrimental effects associated to overstimulation of NMDARs [79], it has been reported that a

persistent increase in D-Asp levels results in the precocious decay of basal glutamatergic transmission, synaptic plasticity, and hippocampal reference memory in mutants [80-82]. Such dysfunctions are mirrored by the loss of excitatory glutamatergic synapses and reduction in synaptic GluN1 and GluN2B subunits [82]. In addition, severe age-dependent neuroinflammation and cell death occur within PFC and hippocampus of *Ddo* knockout animals [81]. On the other hand, increased D-Asp levels in young-adult *Ddo* knockout mice have been associated with improved functional and structural NMDAR-dependent synaptic plasticity. Based on this set of evidence, future studies are mandatory to clarify the impact of D-Asp metabolism in the genetic background of BTBR mice. Nevertheless, it remains unclear whether the broad alterations in D-Asp metabolism found in BTBR mice represent a developmentally relevant contribution or reflect changes occurring only in adulthood. Further experiments on juvenile BTBR mice are needed to investigate this point. It is important also to remark that D-Asp is abundant during brain development [29-31]. In this regard, the recent generation of a mouse model characterized by precocious embryonic D-Asp depletion [31] may help in clarifying the potential involvement of this D-amino acid in a neurodevelopmental disorder like ASD.

Interestingly, we also found higher concentrations of the enantiomer L-Asp in the serum of BTBR mice, thus suggesting an overall peripheral dysregulation of Asp metabolism. In addition to D-Asp, we also found a slight reduction in L-Glu levels in the hippocampus of BTBR mice, along with a substantial increase of this amino acid in the serum. These opposite L-Glu changes might suggest that the observed cerebral and peripheral dysfunctions have separate metabolic origins in the BTBR strain, since this amino acid cannot pass the blood-brain barrier [83]. Remarkably, our observation showing higher L-Glu levels in BTBR serum is consistent with a previous study in humans reporting significantly higher L-Glu serum levels in patients with idiopathic autism [62].

It must be pointed out here that the changes observed in BTBR might somehow be affected by the choice of the comparison strain, namely, C57BL/6J mice. However, such a strain is commonly used for

comparison with BTBR in molecular and behavioral studies [67]. Another limitation is based on the fact that our HPLC analyses were performed on total homogenates. Consequently, we measured the total amount of amino acids without distinguishing between the extracellular fraction and intracellular (neuronal *vs* glial) metabolic pool.

In support of a selective metabolic D-Asp alteration within BTBR brain, all the other three syndromic mouse models of ASD examined did not exhibit gross perturbations in amino acids metabolism in either brain or serum (Table 2). We only found reduced hippocampal content of both D-Asp and L-Asp but unaltered D-Asp/total Asp ratio and *Ddo* gene expression in *Cntnap2*$^{-/-}$ mice. These findings suggest that D-Asp modification observed in *Cntnap2*$^{-/-}$ animals could be an indirect consequence of a regional alteration in L-Asp metabolism. Overall, the results collected in the genetic mouse models of ASD suggest that the single mutations examined, associated to syndromic forms of ASD, are not able to trigger a metabolic D-Asp imbalance in adulthood. Despite D-Asp metabolism selectively changes in BTBR mice, this idiopathic ASD model does not exhibit specific behavioral phenotypes compared to syndromic ASD mouse models [49-52, 84]. Therefore, we cannot predict if specific alterations found in D-Asp metabolism are selectively associated with peculiar BTBR-related ASD phenotypes.

Overall, our findings indicate that metabolic D-Asp dysfunction could represent one of the complex biological components involved in idiopathic forms of ASD. On the other hand, the absence of significant D-Ser changes in all ASD animal models analyzed here does not match with previous biochemical and pharmacological studies in preclinical models and ASD children. Indeed, significant alteration in the serum and urine concentrations of D-Ser and L-Ser has been reported in ASD patients [63, 85-88]. Furthermore, a rescue of behavioural alterations in preclinical models and ASD patients has been demonstrated by improving the occupancy of the glycine B site of NMDARs with D-cycloserine and sarcosine supplementation [89-91]. It is important to remark that our neurochemical analyses were conducted in adult animals while ASD mainly involves neurodevelopmental

dysfunctions that result in clear phenotypes at juvenile stages of life. Remarkably, such juvenile phenotypes differ from those at adulthood at the molecular level [89]. Studies have now established that ASD is associated, at least in animal models, to early hyperfunction of NMDAR before weaning while switching to hypofunction after this period [89]. Based on this consideration, it is conceivable that the lack of any detectable cerebral D-Ser alterations in adult ASD animal models does not imply the absence of any alterations earlier on. Indeed, clinical studies have established that Ser levels are decreased in subjects with ASD [63, 85, 87, 88] and that inhibitors of DAAO such as sodium benzoate could be effective for treating ASD in children, as reported in a pilot trial [91]. Therefore, future investigations are needed to examine the same biochemical measurements both at prenatal and juvenile stages of life.

Another issue that deserves to be deeply investigated in future studies is the potential impact of D-Asp and D-Ser food integration in ASD. In this regard, considering the relevance of food intake on amino acid metabolism, next experiments are mandatory to evaluate whether specific Asp/Ser-deprived or enriched food regime might affect brain and systemic metabolism of ASD mouse models and influence, in turn, their ASD-related phenotypes.

5. Conclusions

In this work, we report that, on top of alterations in L-Glu levels, an idiopathic animal model of ASD, such as BTBR, exhibits robust metabolic perturbation in the NMDAR and mGluR5 agonist D-Asp. This evidence supports on one hand the involvement of an abnormal glutamatergic neurotransmission in the pathophysiology of idiopathic ASD, on the other hand highlight the D-Asp metabolism contribution in the dysfunctional glutamatergic neurotransmission observed in idiopathic ASD.

Acknowledgments: A.U. was supported by a grant from MIUR (Ministero dell'Istruzione, dell'Università e della Ricerca, Progetto PRIN 2017-Project nr 2017M42834). A.G. is supported by the European Research Council (ERC, DISCONN to A.G., Grant Agreement 802371), the Simons Foundation (SFARI 400101), the Brain and Behavior Foundation (NARSAD, #25861), the NIH (1R21MH116473-01A1), Telethon Foundation (GGP19177) and the University of Padua interdepartmental project "Proactive".

References

[1] C. Lord, T.S. Brugha, T. Charman, J. Cusack, G. Dumas, T. Frazier, E.J.H. Jones, R.M. Jones, A. Pickles, M.W. State, J.L. Taylor, J. Veenstra-VanderWeele, Autism spectrum disorder, Nat Rev Dis Primers, 6 (2020) 5.

[2] F.R. Volkmar, D. Pauls, Autism, Lancet, 362 (2003) 1133-1141.

[3] L.M. Iakoucheva, A.R. Muotri, J. Sebat, Getting to the Cores of Autism, Cell, 178 (2019) 1287-1298.

[4] A. Liska, A. Bertero, R. Gomolka, M. Sabbioni, A. Galbusera, N. Barsotti, S. Panzeri, M.L. Scattoni, M. Pasqualetti, A. Gozzi, Homozygous Loss of Autism-Risk Gene CNTNAP2 Results in Reduced Local and Long-Range Prefrontal Functional Connectivity, Cereb Cortex, 28 (2018) 1141-1153.

[5] J.D. Murdoch, M.W. State, Recent developments in the genetics of autism spectrum disorders, Curr Opin Genet Dev, 23 (2013) 310-315.

[6] M. Pagani, A. Bertero, A. Liska, A. Galbusera, M. Sabbioni, N. Barsotti, N. Colenbier, D. Marinazzo, M.L. Scattoni, M. Pasqualetti, A. Gozzi, Deletion of Autism Risk Gene Shank3 Disrupts Prefrontal Connectivity, J Neurosci, 39 (2019) 5299-5310.

[7] A. Bertero, A. Liska, M. Pagani, R. Parolisi, M.E. Masferrer, M. Gritti, M. Pedrazzoli, A. Galbusera, A. Sarica, A. Cerasa, M. Buffelli, R. Tonini, A. Buffo, C. Gross, M. Pasqualetti, A. Gozzi, Autism-associated 16p11.2 microdeletion impairs prefrontal functional connectivity in mouse and human, Brain, 141 (2018) 2055-2065.

[8] J. Horder, M.M. Petrinovic, M.A. Mendez, A. Bruns, T. Takumi, W. Spooren, G.J. Barker, B. Kunnecke, D.G. Murphy, Glutamate and GABA in autism spectrum disorder-a translational magnetic resonance spectroscopy study in man and rodent models, Transl Psychiatry, 8 (2018) 106.

[9] D. Khalifa, O. Shahin, D. Salem, O. Raafat, Serum glutamate was elevated in children aged 3-10 years with autism spectrum disorders when they were compared with controls, Acta Paediatr, 108 (2019) 295-299.

[10] H.F. Zheng, W.Q. Wang, X.M. Li, G. Rauw, G.B. Baker, Body fluid levels of neuroactive amino acids in autism spectrum disorders: a review of the literature, Amino Acids, 49 (2017) 57-65.

[11] E.J. Lee, S.Y. Choi, E. Kim, NMDA receptor dysfunction in autism spectrum disorders, Curr Opin Pharmacol, 20 (2015) 8-13.

[12] E. Moretto, L. Murru, G. Martano, J. Sassone, M. Passafaro, Glutamatergic synapses in neurodevelopmental disorders, Prog Neuropsychopharmacol Biol Psychiatry, 84 (2018) 328-342.

[13] G. Uzunova, E. Hollander, J. Shepherd, The role of ionotropic glutamate receptors in childhood neurodevelopmental disorders: autism spectrum disorders and fragile x syndrome, Curr Neuropharmacol, 12 (2014) 71-98.

[14] R.F. Tzang, C.H. Chang, Y.C. Chang, H.Y. Lane, Autism Associated With Anti-NMDAR Encephalitis: Glutamate-Related Therapy, Front Psychiatry, 10 (2019) 440.

[15] S.W. Hulbert, Y.H. Jiang, Monogenic mouse models of autism spectrum disorders: Common mechanisms and missing links, Neuroscience, 321 (2016) 3-23.

[16] T. Rinaldi, K. Kulangara, K. Antoniello, H. Markram, Elevated NMDA receptor levels and enhanced postsynaptic long-term potentiation induced by prenatal exposure to valproic acid, Proc Natl Acad Sci U S A, 104 (2007) 13501-13506.

[17] M.V. Mehta, M.J. Gandal, S.J. Siegel, mGluR5-antagonist mediated reversal of elevated stereotyped, repetitive behaviors in the VPA model of autism, PLoS One, 6 (2011) e26077.

[18] J.T. Coyle, Glutamate and schizophrenia: beyond the dopamine hypothesis, Cell Mol Neurobiol, 26 (2006) 365-384.

[19] S.L. Grant, Y. Shulman, P. Tibbo, D.R. Hampson, G.B. Baker, Determination of d-serine and related neuroactive amino acids in human plasma by high-performance liquid chromatography with fluorimetric detection, J Chromatogr B Analyt Technol Biomed Life Sci, 844 (2006) 278-282.

[20] V. Labrie, T. Lipina, J.C. Roder, Mice with reduced NMDA receptor glycine affinity model some of the negative and cognitive symptoms of schizophrenia, Psychopharmacology (Berl), 200 (2008) 217-230.

[21] K.S. Lam, M.G. Aman, L.E. Arnold, Neurochemical correlates of autistic disorder: a review of the literature, Res Dev Disabil, 27 (2006) 254-289.

[22] D. Ongur, J.E. Jensen, A.P. Prescot, C. Stork, M. Lundy, B.M. Cohen, P.F. Renshaw, Abnormal glutamatergic neurotransmission and neuronal-glial interactions in acute mania, Biol Psychiatry, 64 (2008) 718-726.

[23] C. Yuksel, D. Ongur, Magnetic resonance spectroscopy studies of glutamate-related abnormalities in mood disorders, Biol Psychiatry, 68 (2010) 785-794.

[24] A.R. Durrant, U. Heresco-Levy, D-Serine in Neuropsychiatric Disorders: New Advances, Advances in Psychiatry, 2014 (2014) 859735.

[25] M. Martineau, G. Baux, J.P. Mothet, D-serine signalling in the brain: friend and foe, Trends Neurosci, 29 (2006) 481-491.

[26] H. Wolosker, D.T. Balu, J.T. Coyle, The Rise and Fall of the d-Serine-Mediated Gliotransmission Hypothesis, Trends Neurosci, 39 (2016) 712-721.

[27] F. Errico, T. Nuzzo, M. Carella, A. Bertolino, A. Usiello, The Emerging Role of Altered d-Aspartate Metabolism in Schizophrenia: New Insights From Preclinical Models and Human Studies, Front Psychiatry, 9 (2018) 559.

[28] G. Molinaro, S. Pietracupa, L. Di Menna, L. Pescatori, A. Usiello, G. Battaglia, F. Nicoletti, V. Bruno, D-aspartate activates mGlu receptors coupled to polyphosphoinositide hydrolysis in neonate rat brain slices, Neurosci Lett, 478 (2010) 128-130.

[29] A. Hashimoto, S. Kumashiro, T. Nishikawa, T. Oka, K. Takahashi, T. Mito, S. Takashima, N. Doi, Y. Mizutani, T. Yamazaki, et al., Embryonic development and postnatal changes in free D-aspartate and D-serine in the human prefrontal cortex, J Neurochem, 61 (1993) 348-351.

[30] D.S. Dunlop, A. Neidle, D. McHale, D.M. Dunlop, A. Lajtha, The presence of free D-aspartic acid in rodents and man, Biochem Biophys Res Commun, 141 (1986) 27-32.

[31] A. De Rosa, F. Mastrostefano, A. Di Maio, T. Nuzzo, Y. Saitoh, M. Katane, A.M. Isidori, V. Caputo, P. Marotta, G. Falco, M.E. De Stefano, H. Homma, A. Usiello, F. Errico, Prenatal expression of D-aspartate oxidase causes early cerebral D-aspartate depletion and influences brain morphology and cognitive functions at adulthood, Amino Acids, 52 (2020) 597-617.

[32] H. Wolosker, D-serine regulation of NMDA receptor activity, Sci STKE, 2006 (2006) pe41.

[33] L. Pollegioni, S. Sacchi, Metabolism of the neuromodulator D-serine, Cell Mol Life Sci, 67 (2010) 2387-2404.

[34] M. Horio, T. Ishima, Y. Fujita, R. Inoue, H. Mori, K. Hashimoto, Decreased levels of free D-aspartic acid in the forebrain of serine racemase (Srr) knock-out mice, Neurochem Int, 62 (2013) 843-847.

[35] T. Ito, M. Hayashida, S. Kobayashi, N. Muto, A. Hayashi, T. Yoshimura, H. Mori, Serine racemase is involved in d-aspartate biosynthesis, J Biochem, 160 (2016) 345-353.

[36] A. Tanaka-Hayashi, S. Hayashi, R. Inoue, T. Ito, K. Konno, T. Yoshida, M. Watanabe, T. Yoshimura, H. Mori, Is D-aspartate produced by glutamic-oxaloacetic transaminase-1 like 1 (Got1l1): a putative aspartate racemase?, Amino Acids, 47 (2015) 79-86.

[37] S. Sacchi, L. Caldinelli, P. Cappelletti, L. Pollegioni, G. Molla, Structure-function relationships in human D-amino acid oxidase, Amino Acids, 43 (2012) 1833-1850.

[38] G. Murtas, S. Sacchi, M. Valentino, L. Pollegioni, Biochemical Properties of Human D-Amino Acid Oxidase, Front Mol Biosci, 4 (2017) 88.

[39] M. Katane, H. Homma, D-aspartate oxidase: the sole catabolic enzyme acting on free D-aspartate in mammals, Chem Biodivers, 7 (2010) 1435-1449.

[40] E.A. Nunes, E.M. MacKenzie, D. Rossolatos, J. Perez-Parada, G.B. Baker, S.M. Dursun, D-serine and schizophrenia: an update, Expert Rev Neurother, 12 (2012) 801-812.

[41] D.T. Balu, J.T. Coyle, The NMDA receptor 'glycine modulatory site' in schizophrenia: D-serine, glycine, and beyond, Curr Opin Pharmacol, 20 (2015) 109-115.

[42] Y. Ozeki, M. Sekine, K. Fujii, T. Watanabe, H. Okuyasu, Y. Takano, T. Shinozaki, A. Aoki, K. Akiyama, H. Homma, K. Shimoda, Phosphoserine phosphatase activity is elevated and correlates negatively with plasma d-serine concentration in patients with schizophrenia, Psychiatry Res, 237 (2016) 344-350.

[43] T. Nuzzo, S. Sacchi, F. Errico, S. Keller, O. Palumbo, E. Florio, D. Punzo, F. Napolitano, M. Copetti, M. Carella, L. Chiariotti, A. Bertolino, L. Pollegioni, A. Usiello, Decreased free d-aspartate levels are linked to enhanced d-aspartate oxidase activity in the dorsolateral prefrontal cortex of schizophrenia patients, NPJ Schizophr, 3 (2017) 16.

[44] J. Yamada, A. Okabe, H. Toyoda, W. Kilb, H.J. Luhmann, A. Fukuda, Cl- uptake promoting depolarizing GABA actions in immature rat neocortical neurones is mediated by NKCC1, J Physiol, 557 (2004) 829-841.

[45] L.J. Young, C.E. Barrett, Neuroscience. Can oxytocin treat autism?, Science, 347 (2015) 825-826.

[46] K. Hashimoto, T. Yoshida, M. Ishikawa, Y. Fujita, T. Niitsu, M. Nakazato, H. Watanabe, T. Sasaki, A. Shiina, T. Hashimoto, N. Kanahara, T. Hasegawa, M. Enohara, A. Kimura, M. Iyo,

Increased serum levels of serine enantiomers in patients with depression, Acta Neuropsychiatr, 28 (2016) 173-178.

[47] L. Deutschenbaur, J. Beck, A. Kiyhankhadiv, M. Muhlhauser, S. Borgwardt, M. Walter, G. Hasler, D. Sollberger, U.E. Lang, Role of calcium, glutamate and NMDA in major depression and therapeutic application, Prog Neuropsychopharmacol Biol Psychiatry, 64 (2016) 325-333.

[48] K. Hashimoto, D. Bruno, J. Nierenberg, C.R. Marmar, H. Zetterberg, K. Blennow, N. Pomara, Abnormality in glutamine-glutamate cycle in the cerebrospinal fluid of cognitively intact elderly individuals with major depressive disorder: a 3-year follow-up study, Transl Psychiatry, 6 (2016) e744.

[49] K.Z. Meyza, D.C. Blanchard, The BTBR mouse model of idiopathic autism – Current view on mechanisms, Neuroscience & Biobehavioral Reviews, 76 (2017) 99-110.

[50] O. Penagarikano, B.-á. Abrahams, E.-á. Herman, K.-á. Winden, A. Gdalyahu, H. Dong, L.-á. Sonnenblick, R. Gruver, J. Almajano, A. Bragin, P. Golshani, J.-á. Trachtenberg, E. Peles, D.-á. Geschwind, Absence of CNTNAP2 Leads to Epilepsy, Neuronal Migration Abnormalities, and Core Autism-Related Deficits, Cell, 147 (2011) 235-246.

[51] J. Peca, C. Feliciano, J.T. Ting, W. Wang, M.F. Wells, T.N. Venkatraman, C.D. Lascola, Z. Fu, G. Feng, Shank3 mutant mice display autistic-like behaviours and striatal dysfunction, Nature, 472 (2011) 437-442.

[52] G. Horev, J. Ellegood, J.P. Lerch, Y.E.E. Son, L. Muthuswamy, H. Vogel, A.M. Krieger, A. Buja, R.M. Henkelman, M. Wigler, A.A. Mills, Dosage-dependent phenotypes in models of 16p11.2 lesions found in autism, Proceedings of the National Academy of Sciences of the United States of America, 108 (2011) 17076-17081.

[53] I. Fernandez, A. Pena, N. Del Teso, V. Perez, J. Rodriguez-Cuesta, Clinical biochemistry parameters in C57BL/6J mice after blood collection from the submandibular vein and retroorbital plexus, J Am Assoc Lab Anim Sci, 49 (2010) 202-206.

[54] Z. Long, N. Nimura, M. Adachi, M. Sekine, T. Hanai, H. Kubo, H. Homma, Determination of D- and L-aspartate in cell culturing medium, within cells of MPT1 cell line and in rat blood by a column-switching high-performance liquid chromatogrpahic method, J Chromatogr B Biomed Sci Appl, 761 (2001) 99-106.

[55] T. Nuzzo, D. Punzo, P. Devoto, E. Rosini, S. Paciotti, S. Sacchi, Q. Li, M.L. Thiolat, C. Vega, M. Carella, M. Carta, F. Gardoni, P. Calabresi, L. Pollegioni, E. Bezard, L. Parnetti, F. Errico, A. Usiello, The levels of the NMDA receptor co-agonist D-serine are reduced in the substantia nigra of MPTP-lesioned macaques and in the cerebrospinal fluid of Parkinson's disease patients, Sci Rep, 9 (2019) 8898.

[56] M. Katane, H. Kuwabara, K. Nakayama, Y. Saitoh, T. Miyamoto, M. Sekine, H. Homma, Rat d-aspartate oxidase is more similar to the human enzyme than the mouse enzyme, Biochim Biophys Acta Proteins Proteom, 1866 (2018) 806-812.

[57] M. Katane, R. Kanazawa, R. Kobayashi, M. Oishi, K. Nakayama, Y. Saitoh, T. Miyamoto, M. Sekine, H. Homma, Structure-function relationships in human d-aspartate oxidase: characterisation of variants corresponding to known single nucleotide polymorphisms, Biochim Biophys Acta Proteins Proteom, 1865 (2017) 1129-1140.

[58] J.L. Silverman, J.N. Crawley, The promising trajectory of autism therapeutics discovery, Drug Discov Today, 19 (2014) 838-844.

[59] H. Wei, C. Dobkin, A.M. Sheikh, M. Malik, W.T. Brown, X. Li, The therapeutic effect of memantine through the stimulation of synapse formation and dendritic spine maturation in autism and fragile X syndrome, PLoS One, 7 (2012) e36981.

[60] D.C. Rojas, The role of glutamate and its receptors in autism and the use of glutamate receptor antagonists in treatment, J Neural Transm (Vienna), 121 (2014) 891-905.

[61] L.K. Fung, A.Y. Hardan, Developing Medications Targeting Glutamatergic Dysfunction in Autism: Progress to Date, CNS Drugs, 29 (2015) 453-463.

[62] A. Shinohe, K. Hashimoto, K. Nakamura, M. Tsujii, Y. Iwata, K.J. Tsuchiya, Y. Sekine, S. Suda, K. Suzuki, G. Sugihara, H. Matsuzaki, Y. Minabe, T. Sugiyama, M. Kawai, M. Iyo, N. Takei, N. Mori, Increased serum levels of glutamate in adult patients with autism, Prog Neuropsychopharmacol Biol Psychiatry, 30 (2006) 1472-1477.

[63] R. Tirouvanziam, T.V. Obukhanych, J. Laval, P.A. Aronov, P. Libove, A.G. Banerjee, K.J. Parker, R. O'Hara, L.A. Herzenberg, L.A. Herzenberg, A.Y. Hardan, Distinct plasma profile of polar neutral amino acids, leucine, and glutamate in children with Autism Spectrum Disorders, J Autism Dev Disord, 42 (2012) 827-836.

[64] C. Shimmura, S. Suda, K.J. Tsuchiya, K. Hashimoto, K. Ohno, H. Matsuzaki, K. Iwata, K. Matsumoto, T. Wakuda, Y. Kameno, K. Suzuki, M. Tsujii, K. Nakamura, N. Takei, N. Mori, Alteration of plasma glutamate and glutamine levels in children with high-functioning autism, PLoS One, 6 (2011) e25340.

[65] C. Shimmura, K. Suzuki, Y. Iwata, K.J. Tsuchiya, K. Ohno, H. Matsuzaki, K. Iwata, Y. Kameno, T. Takahashi, T. Wakuda, K. Nakamura, K. Hashimoto, N. Mori, Enzymes in the glutamate-glutamine cycle in the anterior cingulate cortex in postmortem brain of subjects with autism, Mol Autism, 4 (2013) 6.

[66] K.K. Chadman, S.R. Guariglia, J.H. Yoo, New directions in the treatment of autism spectrum disorders from animal model research, Expert Opin Drug Discov, 7 (2012) 407-416.

[67] J.L. Silverman, M. Yang, C. Lord, J.N. Crawley, Behavioural phenotyping assays for mouse models of autism, Nat Rev Neurosci, 11 (2010) 490-502.

[68] F. Sforazzini, A. Berterto, L. Dodero, G. David, A. Galbusera, A. Bifone, M.L. Scattoni, M. Pasqualetti, A. Gozzi, Erratum to: Altered functional connectivity networks in acallosal and socially impaired BTBR mice, Brain Struct Funct, 221 (2016) 1207.

[69] D.M. Jones-Davis, M. Yang, E. Rider, N.C. Osbun, G.J. da Gente, J. Li, A.M. Katz, M.D. Weber, S. Sen, J. Crawley, E.H. Sherr, Quantitative trait loci for interhemispheric commissure development and social behaviors in the BTBR T(+) tf/J mouse model of autism, PLoS One, 8 (2013) e61829.

[70] M.L. Scattoni, S.U. Gandhy, L. Ricceri, J.N. Crawley, Unusual repertoire of vocalizations in the BTBR T+tf/J mouse model of autism, PLoS One, 3 (2008) e3067.

[71] M.L. Scattoni, A. Martire, G. Cartocci, A. Ferrante, L. Ricceri, Reduced social interaction, behavioural flexibility and BDNF signalling in the BTBR T+ tf/J strain, a mouse model of autism, Behav Brain Res, 251 (2013) 35-40.

[72] D. Wahlsten, P. Metten, J.C. Crabbe, Survey of 21 inbred mouse strains in two laboratories reveals that BTBR T/+ tf/tf has severely reduced hippocampal commissure and absent corpus callosum, Brain Res, 971 (2003) 47-54.

[73] M. Squillace, L. Dodero, M. Federici, S. Migliarini, F. Errico, F. Napolitano, P. Krashia, A. Di Maio, A. Galbusera, A. Bifone, M.L. Scattoni, M. Pasqualetti, N.B. Mercuri, A. Usiello, A. Gozzi, Dysfunctional dopaminergic neurotransmission in asocial BTBR mice, Transl Psychiatry, 4 (2014) e427.

[74] B. Egaas, E. Courchesne, O. Saitoh, Reduced size of corpus callosum in autism, Arch Neurol, 52 (1995) 794-801.

[75] A.L. Alexander, J.E. Lee, M. Lazar, R. Boudos, M.B. DuBray, T.R. Oakes, J.N. Miller, J. Lu, E.K. Jeong, W.M. McMahon, E.D. Bigler, J.E. Lainhart, Diffusion tensor imaging of the corpus callosum in Autism, Neuroimage, 34 (2007) 61-73.

[76] G. Provenzano, Z. Corradi, K. Monsorno, T. Fedrizzi, L. Ricceri, M.L. Scattoni, Y. Bozzi, Comparative Gene Expression Analysis of Two Mouse Models of Autism: Transcriptome Profiling of the BTBR and En2 (-/-) Hippocampus, Front Neurosci, 10 (2016) 396.

[77] H. Wolosker, K.N. Sheth, M. Takahashi, J.P. Mothet, R.O. Brady, Jr., C.D. Ferris, S.H. Snyder, Purification of serine racemase: biosynthesis of the neuromodulator D-serine, Proceedings of the National Academy of Sciences of the United States of America, 96 (1999) 721-725.

[78] F. Errico, M.T. Pirro, A. Affuso, P. Spinelli, M. De Felice, A. D'Aniello, R. Di Lauro, A physiological mechanism to regulate D-aspartic acid and NMDA levels in mammals revealed by D-aspartate oxidase deficient mice, Gene, 374 (2006) 50-57.

[79] G.E. Hardingham, H. Bading, The Yin and Yang of NMDA receptor signalling, Trends Neurosci, 26 (2003) 81-89.

[80] F. Errico, R. Nistico, F. Napolitano, C. Mazzola, D. Astone, T. Pisapia, M. Giustizieri, A. D'Aniello, N.B. Mercuri, A. Usiello, Increased D-aspartate brain content rescues hippocampal age-related synaptic plasticity deterioration of mice, Neurobiol Aging, 32 (2011) 2229-2243.

[81] D. Punzo, F. Errico, L. Cristino, S. Sacchi, S. Keller, C. Belardo, L. Luongo, T. Nuzzo, R. Imperatore, E. Florio, V. De Novellis, O. Affinito, S. Migliarini, G. Maddaloni, M.J. Sisalli, M. Pasqualetti, L. Pollegioni, S. Maione, L. Chiariotti, A. Usiello, Age-Related Changes in D-Aspartate Oxidase Promoter Methylation Control Extracellular D-Aspartate Levels and Prevent Precocious Cell Death during Brain Aging, J Neurosci, 36 (2016) 3064-3078.

[82] L. Cristino, L. Luongo, M. Squillace, G. Paolone, D. Mango, S. Piccinin, E. Zianni, R. Imperatore, M. Iannotta, F. Longo, F. Errico, A.L. Vescovi, M. Morari, S. Maione, F. Gardoni, R. Nistico, A. Usiello, d-Aspartate oxidase influences glutamatergic system homeostasis in mammalian brain, Neurobiol Aging, 36 (2015) 1890-1902.

[83] A.L. Sheldon, M.B. Robinson, The role of glutamate transporters in neurodegenerative diseases and potential opportunities for intervention, Neurochem Int, 51 (2007) 333-355.

[84] T.M. Kazdoba, P.T. Leach, M. Yang, J.L. Silverman, M. Solomon, J.N. Crawley, Translational Mouse Models of Autism: Advancing Toward Pharmacological Therapeutics, Curr Top Behav Neurosci, 28 (2016) 1-52.

[85] J. Kaluzna-Czaplinska, E. Zurawicz, W. Struck, M. Markuszewski, Identification of organic acids as potential biomarkers in the urine of autistic children using gas chromatography/mass spectrometry, J Chromatogr B Analyt Technol Biomed Life Sci, 966 (2014) 70-76.

[86] A. Noto, V. Fanos, L. Barberini, D. Grapov, C. Fattuoni, M. Zaffanello, A. Casanova, G. Fenu, A. De Giacomo, M. De Angelis, C. Moretti, P. Papoff, P. Ditonno, R. Francavilla, The urinary metabolomics profile of an Italian autistic children population and their unaffected siblings, J Matern Fetal Neonatal Med, 27 Suppl 2 (2014) 46-52.

[87] C. Evans, R.H. Dunstan, T. Rothkirch, T.K. Roberts, K.L. Reichelt, R. Cosford, G. Deed, L.B. Ellis, D.L. Sparkes, Altered amino acid excretion in children with autism, Nutr Neurosci, 11 (2008) 9-17.

[88] X. Ming, T.P. Stein, V. Barnes, N. Rhodes, L. Guo, Metabolic perturbance in autism spectrum disorders: a metabolomics study, J Proteome Res, 11 (2012) 5856-5862.

[89] C. Chung, S. Ha, H. Kang, J. Lee, S.M. Um, H. Yan, Y.E. Yoo, T. Yoo, H. Jung, D. Lee, E. Lee, S. Lee, J. Kim, R. Kim, Y. Kwon, W. Kim, H. Kim, L. Duffney, D. Kim, W. Mah, H. Won, S. Mo, J.Y. Kim, C.S. Lim, B.K. Kaang, T.M. Boeckers, Y. Chung, H. Kim, Y.H. Jiang, E. Kim, Early Correction of N-Methyl-D-Aspartate Receptor Function Improves Autistic-like Social Behaviors in Adult Shank2(-/-) Mice, Biol Psychiatry, 85 (2019) 534-543.

[90] M. Urbano, L. Okwara, P. Manser, K. Hartmann, A. Herndon, S.I. Deutsch, A trial of D-cycloserine to treat stereotypies in older adolescents and young adults with autism spectrum disorder, Clin Neuropharmacol, 37 (2014) 69-72.

[91] P.J.T.M. Yang, A Pilot Trial of Sodium Benzoate, a D-Amino Acid Oxidase Inhibitor, Added on Augmentative and Alternative Communication Intervention for Non-Communicative Children with Autism Spectrum Disorders, 6 (2017) 1-5.

Figure Legends

Figure 1. *HPLC detection of free D-aspartate and L-aspartate content in the prefrontal cortex of BTBR, Cntnap2$^{-/-}$, Shank3$^{-/-}$ and 16p11.2$^{+/-}$ mice*. (**a- c**) Analysis of (a) D-aspartate, (b) L-aspartate levels and (c) D-/total aspartate ratio in the prefrontal cortex of BTBR and C57BL6/J strains (n=4/strain). (**d-f**) Amount of (d) D-aspartate, (e) L-aspartate, and (f) D-/total aspartate ratio in the prefrontal cortex of *Cntnap2*$^{-/-}$ and *Cntnap2*$^{+/+}$ mice (n=4/genotype) determined by HPLC analysis. (**g-i**) Measurement of (g) D-aspartate, (h) L-aspartate content, and (i) D-/total aspartate ratio in the prefrontal cortex of *Shank3*$^{-/-}$ (n=3) and *Shank3*$^{+/+}$ (n=4) animals. (**j-l**) Analysis of levels of (j) D-aspartate, (k) L-aspartate, and (l) D-/total Asp ratio in the prefrontal cortex of *16p11.2*$^{+/-}$ mutants and *16p11.2*$^{+/+}$ rodents (n=4/genotype). **p*<0.05, ***p < 0.0001 (Aspin-Welch's test analysis). Values are expressed as the mean±SEM. All the amino acids were detected in a single run by HPLC and expressed as nmol/g tissue, while the ratio is expressed as percentage (%).

Figure 2. *HPLC detection of free D-aspartate and L-aspartate content in the hippocampus of BTBR, Cntnap2$^{-/-}$, Shank3$^{-/-}$ and 16p11.2$^{+/-}$ mice*. (**a- c**) Analysis of (a) D-aspartate, (b) L-aspartate levels and (c) D-/total aspartate ratio in the hippocampus of BTBR and C57BL6/J strains (n=4/strain). (**d-f**) Amount of (d) D-aspartate, (e) L-aspartate, and (f) D-/total aspartate ratio in the hippocampus of *Cntnap2*$^{-/-}$ and *Cntnap2*$^{+/+}$ mice (n=4/genotype) determined by HPLC analysis. (**g-i**) Measurement of (g) D-aspartate, (h) L-aspartate content, and (i) D-/total aspartate ratio in the hippocampus of *Shank3*$^{-/-}$ (n=3) and *Shank3*$^{+/+}$ (n=4) animals. (**j-l**) Analysis of levels of (j) D-aspartate, (k) L-aspartate, and (l) D-/total Asp ratio in the hippocampus of *16p11.2*$^{+/-}$ mutants and *16p11.2*$^{+/+}$ rodents (n=4/genotype). **p*<0.05, ***p < 0.0001 (Aspin-Welch's test analysis). Values are expressed as the mean±SEM. All the amino acids were detected in a single run by HPLC and expressed as nmol/g tissue, while the ratio is expressed as percentage (%).

Figure 3. *HPLC detection of free D-aspartate and L-aspartate content in the serum of BTBR, Cntnap2$^{-/-}$, Shank3$^{-/-}$ and 16p11.2$^{+/-}$ mice*. (**a- c**) Analysis of (a) D-aspartate, (b) L-aspartate levels and (c) D-/total aspartate ratio in the serum of BTBR and C57BL6/J strains (n=4/strain). (**d-f**) Amount of (d) D-aspartate, (e) L-aspartate, and (f) D-/total aspartate ratio in the serum of *Cntnap2*$^{-/-}$ and *Cntnap2*$^{+/+}$ mice (n=4/genotype) determined by HPLC analysis. (**g-i**) Measurement of (g) D-aspartate, (h) L-aspartate content, and (i) D-/total aspartate ratio in the serum of *Shank3*$^{-/-}$ (n=3) and *Shank3*$^{+/+}$ (n=4) animals. (**j-l**) Analysis of levels of (j) D-aspartate, (k) L-aspartate, and (l) D-/total Asp ratio in the serum of *16p11.2*$^{+/-}$ mutants and *16p11.2*$^{+/+}$ rodents (n=4/genotype). **p*<0.05 (Aspin-Welch's test analysis). Values are expressed as the mean±SEM. All the amino acids were detected in a single run by HPLC and expressed as nmol/g tissue, while the ratio is expressed as percentage (%).

Figure 4. *L-glutamate levels in the prefrontal cortex, hippocampus, and serum of BTBR, Cntnap2$^{-/-}$, Shank3$^{-/-}$ and 16p11.2$^{+/-}$ mice*. (**a,e,i**) Content of L-glutamate in the (a) prefrontal cortex (n=4/genotype), (e) hippocampus (n=6/genotype), and (i) serum (n=4/genotype) of BTBR and C57BL6/J mice detected by HPLC. (**b,f,j**) L-glutamate amount in the (b) prefrontal cortex (n=4/genotype), (f) hippocampus (n=6/genotype), and (j) serum (n=4/genotype) of *Cntnap2*$^{-/-}$ and *Cntnap2*$^{+/+}$ mice. (**c,g,k**) Detection of L-glutamate content in the (c) prefrontal cortex (*Shank3*$^{+/+}$, n=4; *Shank3*$^{-/-}$, n=3), (g) hippocampus (n=3/genotype), and (k) serum (n=4; *Shank3*$^{-/-}$, n=3) of *Shank3*$^{-/-}$ and wild-type mice. (**d,h,l**) Levels of L-glutamate in the (d) prefrontal cortex (n=4/genotype), (h) hippocampus (n=6/genotype), and (l) serum (n=4/genotype) of *16p11.2*$^{+/-}$ and wild-type *16p11.2*$^{+/+}$ mice. **p*<0.05, compared to control group (Aspin-Welch's test). Values are expressed as the mean±SEM of nmol/g tissue or µM concentrations, while the ratio is expressed as percentage (%).

Figure 5. *Analysis of Ddo, Daao* and *Sr mRNA expression in the brain of BTBR, Cntnap2*$^{-/-}$, *Shank3*$^{-/-}$, *and 16p11.2*$^{+/-}$ *mice.* (**a-f**) Levels of (a,d) *Ddo,* (b,e) *Daao,* and (c,f) *Sr* mRNA expression in the (a- c) prefrontal cortex and (d-f) hippocampus of BTBR and C57BL/6J mice detected by qPCR analysis (n=6/genotype). (**g-l**) Amount of (g,j) *Ddo,* (h,k) *Daao,* and (i,l) *Sr* transcript in the (g-i) prefrontal cortex and (j-l) hippocampus of *Cntnap2*$^{-/-}$ and *Cntnap2*$^{+/+}$ mice (n=6/genotype). (**m-r**) qPCR analysis of (m,p) *Ddo,* (n,q) *Daao,* and (o,r) *Sr* genes in the (m-o) prefrontal cortex and (p-r) hippocampus of *Shank3*$^{-/-}$ and *Shank3*$^{+/+}$ animals (n=9/genotype). (**s-x**) Expression levels of (s,v) *Ddo,* (t,x) *Daao,* and (u,x) *Sr* genes in the (s-u) prefrontal cortex and (v-x) hippocampus of *16p11.2*$^{+/-}$ and *16p11.2*$^{+/+}$ (n=12/genotype). N.D. indicates that mRNA expression level was not detectable. mRNA expression for each single gene was normalized to the mean of two housekeeping genes and expressed as $2^{-\Delta\Delta Ct}$. * $p<0.05$, ** $p<0.01$, *** $p<0,0001$ compared to control group (unpaired t-test). All values are expressed as mean ± SEM

Table 1. The mean values of D-serine, L-serine (expressed as nmol/g tissue or µM) and D-serine/total serine (expressed as %) in th prefrontal cortex, hippocampus and serum of BTBR, *Cntnap2*$^{-/-}$, *Shank3*$^{-/-}$ and *16p11.2*$^{+/-}$ mice are compared to their matched control All values are expressed as mean ± SEM. Statistical analyses are performed by Aspin-Welch's test. Abbreviations: D-Ser = D-serine; L Ser = L-serine.

		C57BL/6J (n=4)		**BTBR** (n=4)	*p value*	***Cntnap2*$^{+/+}$** *(n=4)*		***Cntnap2*$^{-/-}$** *(n=4)*	*p value*	***Shank3*$^{+/+}$** (n=4)		***Shank3*$^{-/-}$** (n=3)	*p value*	**16p11.2$^{+/+}$** (n=4)		**16p11.2$^{+/-}$** (n=4)	*p value*
Prefrontal cortex	D-Ser (nmol/g tissue)	231.89 ± 45.86	*vs*	219.08 ± 59.48	*0,871*	259.26 ± 122.74	*vs*	338.90 ± 68.88	*0,597*	257.22 ± 73.48	*vs*	394.06 ± 27.17	*0,160*	350.93 ± 61.56	*vs*	278.13 ± 92.30	*0,540*
	L-Ser (nmol/g tissue)	500.75 ± 99.72	*vs*	530.16 ± 147.21	*0,875*	590.26 ± 258.06	*vs*	774.24 ± 151.42	*0,566*	606.70 ± 203.7[illegible]	*vs*	876.85 ± 70.25	*0,284*	746.47 ± 123.38	*vs*	575.45 ± 188.09	*0,480*
	D-Ser/Total Ser (%)	31.74 ± 0.45	*vs*	29.36 ± 0.45	*0,009*	29.64 ± 1.29	*vs*	30.35 ± 0.42	*0,631*	[illegible] ± 0.[illegible]	*vs*	31.04 ± 0.58	*0,693*	32.00 ± 0.88	*vs*	32.33 ± 0.37	*0,744*
Hippocampus	D-Ser (nmol/g tissue)	285.64 ± 79.66	*vs*	390.55 ± 65.95	*0,351*	404.26 ± 68.43	*vs*	233.30 ± 39.04	*0,08[illegible]*	25[illegible].11 ± 105.94	*vs*	268.30 ± 83.51	*0,937*	296.61 ± 71.09	*vs*	239.83 ± 47.03	*0,534*
	L-Ser (nmol/g tissue)	791.07 ± 225.97	*vs*	1114.05 ± 209.79	*0,335*	1114.15 ± 212.41	*vs*	621.16 ± [illegible].4	*0,101*	691.66 ± 272.79	*vs*	725.54 ± 247.52	*0,930*	805.00 ± 218.69	*vs*	636.60 ± 133.21	*0,540*
	D-Ser/Total Ser (%)	26.61 ± 0.18	*vs*	26.17 ± 0.43	*0,393*	26.87 ± 0.59	*vs*	[illegible] ± 0.39	*0,447*	26.80 ± 0.37	*vs*	27.33 ± 0.67	*0,542*	27.28 ± 0.56	*vs*	27.54 ± 0.42	*0,723*
Serum	D-Ser (µM)	1.65 ± 0.63	*vs*	2.62 ± 0.03	*0,224*	2.36 ± 0.[illegible]	*vs*	2.24 ± 0.43	*0,842*	3.41 ± 0.27	*vs*	3.83 ± 0.72	*0,636*	2.92 ± 0.56	*vs*	1.75 ± 0.55	*0,187*
	L-Ser (µM)	115.65 ± 32.02	*vs*	148.75 ± 8.82	*0,384*	12[illegible].75 ± 14.[illegible]	*vs*	155.61 ± 23.43	*0,287*	180.07 ± 19.68	*vs*	31.97	*0,839*	104.53 ± 6.47	*vs*	90.46 ± 22.27	*0,581*
	D-Ser/Total Ser (%)	1.28 ± 0.15	*vs*	1.75 ± 0.12	*0,053*	1.87 ± 0.12	*vs*	1.40 ± 0.12	*0,036*	1.96 ± 0.33	*vs*	2.18 ± 0.01	*0,573*	2.78 ± 0.60	*vs*	1.81 ± 0.22	*0,208*

Table 2. Schematic representation of D-Asp metabolism in the prefrontal cortex, hippocampus and serum of ASD mouse models. Abbreviations: ↑, increased; ↓, decreased; =, unaltered.

	Prefrontal cortex		**Hippocampus**		**Serum**
ASD mouse model	D-Asp/total Asp	*Ddo* mRNA levels	D-Asp/total Asp	*Ddo* mRNA levels	D-Asp/total Asp
BTBR	↑	↓	↑	↓	↑
***Cntnap2*$^{-/-}$**	=	=	=	=	=
***Shank3*$^{-/-}$**	=	=	=	=	=
***16p11.2*$^{+/-}$**	=	=	=	=	=

CRediT author statement

Tommaso Nuzzo: Investigation, Visualization, Formal analysis, Writing - Review & Editing **Masae Sekine**: Investigation, Visualization **Daniela Punzo**: Investigation, Validation **Mattia Miroballo**: Investigation, Visualization **Masumi Katane**: Resources, Validation, Writing - Review & Editing **Yasuaki Saitoh**: Investigation, Visualization **Alberto Galbusera**: Writing - Review & Editing **Massimo Pasqualetti**: Writing - Review & Editing **Francesco Errico**: Validation, Writing - Review & Editing **Alessandro Gozzi**: Resources, Writing - Review & Editing **Jean-Pierre Mothet**: Writing - Review & Editing **Hiroshi Homma**: Resources, Writing - Review & Editing; Supervision **Alessandro Usiello**: Conceptualization, Writing - Original Draft, Supervision, Funding acquisition

Highlights

- D-aspartate content was increased in the brain and serum of BTBR mice.
- *Ddo* mRNA levels were reduced in prefrontal cortex and hippocampus of BTBR mice.
- D-aspartate metabolism was unaltered in *Cntnap2*$^{-/-}$, *Shank3*$^{-/-}$, and *16p11.2*$^{+/-}$ mice.
- L-glutamate levels were augmented in the serum of BTBR mice.
- D-Ser metabolism was unaltered in BTBR, *Cntnap2*$^{-/-}$, *Shank3*$^{-/-}$ and *16p11.2*$^{+/-}$ mice.